



Local strain energy density for the fatigue assessment of hot dip galvanized welded joints: some recent outcomes

M. Peron, S.M.J. Razavi, F. Berto, J. Torgersen, F. Mutignani

Department of Mechanical and Industrial Engineering, Norwegian University of Science and Technology (NTNU), Richard Birkelands vei 2b, 7491, Trondheim, Norway.

mirco.peron@ntnu.no, javad.razavi@ntnu.no, filippo.berto@ntnu.no, jan.torgersen@ntnu.no

ABSTRACT. Since in literature only data about the effect of the hot-dip galvanizing coating on fatigue behavior of unnotched specimens are available, whereas very few for notched components and none for welded joints, the aim of this paper is to partially fill this lack of knowledge comparing fatigue strength of uncoated and hot-dip galvanized fillet welded cruciform joints made of structural steel S355 welded joints, subjected to a load cycle $R = 0.34$. The results are shown in terms of stress range $\Delta\sigma$ and of the averaged strain energy density range $\Delta\bar{W}$ in a control volume of radius $R_0 = 0.28$ mm

KEYWORDS. Hot-dip galvanized steel; High cycle fatigue; Fillet welded cruciform joint; SED.



Citation: Peron, M., Razavi, S.M.J., Berto, F., Torgersen, J., Mutignani, F., Local strain energy density for the fatigue assessment of hot dip galvanized welded joints: some recent outcomes, *Frattura ed Integrità Strutturale*, 42 (2017) 205-213.

Received: 15.07.2017

Accepted: 31.07.2017

Published: 01.20.2017

Copyright: © 2017 This is an open access article under the terms of the CC-BY 4.0, which permits unrestricted use, distribution, and reproduction in any medium, provided the original author and source are credited.

INTRODUCTION

Corrosion is one of the main issue affecting metallic materials such as iron and steel, and several technique to prevent corrosion are available in literature, especially surface treatments. Among all, hot-dip galvanizing has been widely used, with great successes in a large amount of worldwide applications.

Hot-dip galvanization involves the coating of the base material with a zinc layer and several works investigate the influence of different bath composition on mechanical properties [1, 2] and the effect of this protective film on static and fatigue behavior. Whilst tensile properties are not greatly affect, except for the yield stress, fatigue strength is reported to be reduced when the coating thickness exceed a threshold value [3], calculated employing the Kitagawa–Takahashi diagram. Moreover, Bergengren and Melander [4], found an increase in the detrimental effect on fatigue life increasing the zinc layer thickness, but, nevertheless, contrasting results were obtained by Browne et al., [5], and Nilsson et al., [6], that did not find any correlation in terms of loss of the fatigue strength due to the coating thickness. Furthermore, hot-dip galvanization is still an attractive topic, as proved by several recent studies, such as [7-10]. However, the works just mentioned refer to unnotched specimens and very few results are available for notched components. In fact, at the best of author's knowledge the only data available in literature for notched components are due to Huhn and Valtinat [11], that examined S 235 JR G2 plates with holes and bearing-type connections with punched and drilled holes. Besides this lack of

experimental results on notched components, that represents a great gap since notches greatly affect the mechanical behavior [12–15], the detrimental effect of the zinc layer on the fatigue strength cannot be quantified yet, neither in [11], since a direct comparison between uncoated and hot-dip galvanized notched specimens was not performed. Furthermore, though hot-dip galvanization is widely used to enhance the corrosion resistance of welded joints, none researchers have interested in assessing the effect of this surface treatment on their fatigue behavior.

Thus, the aim of this work is to fill these lacks, by means of experimental fatigue tests on uncoated and hot-dip galvanized fillet welded cruciform joints made of structural steel S355. The results report the harmful effect of the presence of zinc layer on fatigue strength both in terms of stress range $\Delta\sigma$ and of the averaged strain energy density range $\Delta\bar{W}$ in a control volume of radius $R_0 = 0.28$ mm.

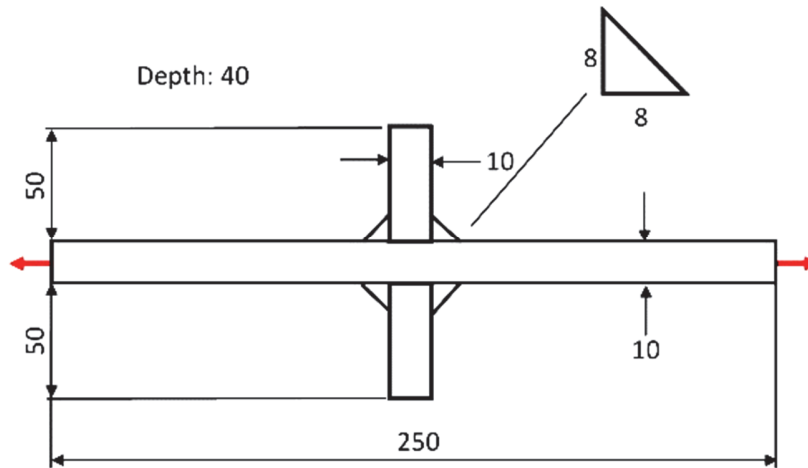


Figure 1: Geometry of the fillet welded cruciform specimen and typical fracture surface.

EXPERIMENTAL DETAILS

The steel plates used to fabricate the samples were 10 mm in thickness, while the complete specimen had a global length of 250 mm. The complete geometry of the specimen can be seen in Fig. 1. Fatigue tests have been conducted on transverse non-load carrying fillet welded joints, made of S 355J2+N structural steel. Welding beads have been made by means of automatic MAG (Metal Active Gas) technique. One of the two series of welded joints has been later hot dip galvanized. Tests have been performed on a servo-hydraulic MTS 810 test system with a load cell capacity of 250 kN at 10 Hz frequency, in air, at room temperature. All samples have been tested using a sinusoidal signal in uniaxial tension (plane loading) and a load ratio $R = 0$, under remote force control. Regarding the galvanized series, the coating treatment has been carried out at a bath temperature of 452 °C and the immersion time was kept equal to 4 minutes for all the specimens. As a consequence, the coating thickness resulted in a range between 96 and 104 μm .

RESULTS

Fatigue tests results are here presented in terms of the stress range $\Delta\sigma = \sigma_{max} - \sigma_{min}$ versus the number of cycles to failure, in a double logarithmic scale. The stress range is referred to the nominal area (400 mm²). Failure has always occurred at the weld toe, as expected, with a typical fracture surface as that shown in Fig. 1. The results from the tests were statistically elaborated by using a log-normal distribution. The ‘run-out’ samples, over two million cycles, were not included in the statistical analysis and are marked in the graphs with an arrow. Fig. 2 refers to uncoated and coated series, while Fig. 3 shows all the data elaborated together: in addition to the mean curve relative to a survival probability of $P_s = 50\%$, (Wöhler curve) the scatter band defined by lines with 10% and 90% of probability of survival (Haibach scatter band) is also plotted. The mean stress amplitude values corresponding to two million cycles, the inverse slope k value of the Wöhler curve and the scatter index T_σ (the ratio between the stress amplitudes corresponding to 10% and 90% of survival probability) are provided in the figure. For the complete listing of the results of the fatigue tests, please refer to Tab. 1.



It can be noted, comparing the uncoated and coated series (Fig. 2), that the scatter index reduces from 1.6 to 1.3. This value is reasonably low both for the uncoated series and the galvanized one. Moreover also in terms of fatigue strength the effect of the galvanization is found to be negligible with a reduction, at $N = 2 \times 10^6$ and $P_s = 90\%$, from 83 to 82 MPa. Furthermore, from the data summarised in Fig. 3, it is possible to see that the fatigue strength at $N = 2 \times 10^6$ and $P_s = 90\%$ is 75 MPa: this value is comparable with the fatigue stress range (from 71 to 80 MPa) given for the corresponding detail category in Eurocode 3.

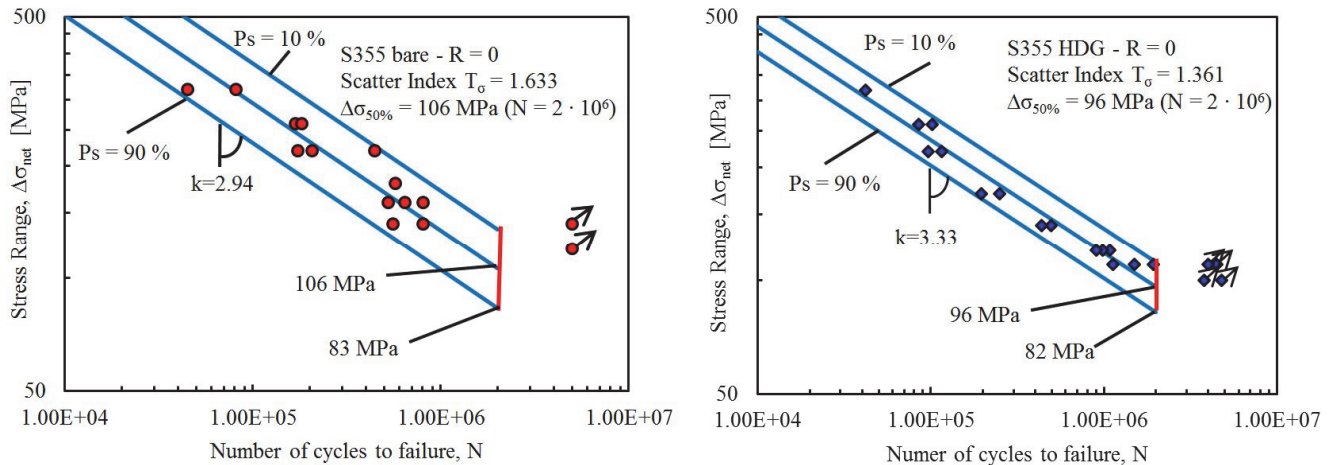


Figure 2: Fatigue behaviour of bare (left) and galvanized (HDG, right) welded steel at $R = 0$.

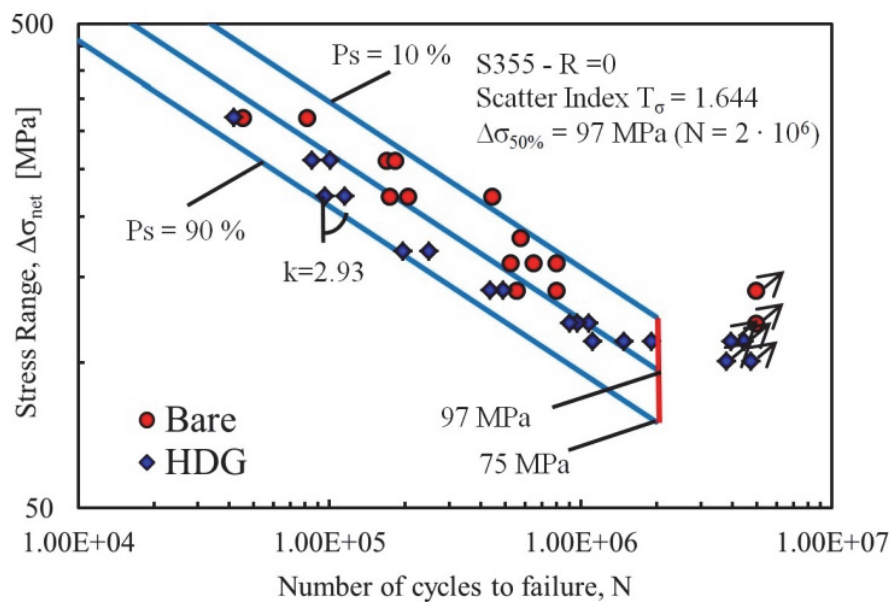


Figure 3: Fatigue behaviour of both uncoated and galvanized welded steel at $R = 0$.

STRAIN ENERGY DENSITY APPROACH

An averaged strain energy density (SED) criterion has been proposed and formalized first by Lazzarin and Zambardi ([16]), and later has been extensively studied and applied for static failures and fatigue life assessment of notched and welded components subjected to different loading conditions [17]. According to this volume-based criterion, the failure occurs when the mean value of the strain energy density \bar{W} over a control volume with a well-

defined radius R_0 is equal to a critical value W_C , which does not depend on the notch sharpness. The critical value and the radius of the control volume (which becomes an area in bi-dimensional problems) are dependent on the material [17].

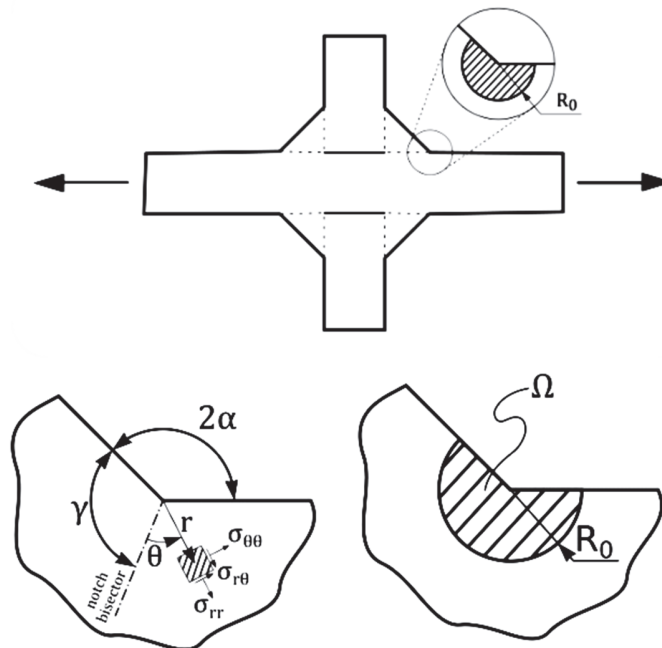


Figure 4: Polar coordinate system and critical volume (area) centered at the notch tip.

UNCOATED SPECIMENS			COATED SPECIMENS		
$\Delta\sigma$ [MPa]	N [cycles]	$\Delta\bar{W}$ [N.mm/mm ³]	$\Delta\sigma$ [MPa]	N [cycles]	$\Delta\bar{W}$ [N.mm/mm ³]
260	168750	0.5692	140	494000	0.1650
320	81500	0.8622	120	1079000	0.1212
260	181484	0.5692	100	4800000	<i>Run out</i> 0.0842
220	445750	0.4075	260	85000	0.5692
180	572333	0.2728	140	436500	0.1650
140	5000000	<i>Run out</i> 0.1650	120	978200	0.1212
160	803000	0.2155	220	96820	0.4075
160	523983	0.2155	120	905500	0.1212
140	804960	0.1650	110	1125546	0.1019
140	556990	0.1650	100	3800000	<i>Run out</i> 0.0842
160	645140	0.2155	110	1500000	0.1019
320	45000	0.8622	110	4500000	<i>Run out</i> 0.1019
120	5000000	<i>Run out</i> 0.1212	110	4000000	<i>Run out</i> 0.1019
220	173000	0.4075	260	101200	0.5692
220	205616	0.4075	170	195000	0.2433
			170	250000	0.2433
			110	1940000	0.1019
			320	42000	0.8622
			220	115000	0.4075

Table 1: Fatigue results from uncoated and coated (HDG) welded specimens.

The SED approach was formalized and applied first to sharp, zero radius, V-notches ([16]), considering bi-dimensional problems (plane stress or plane strain hypothesis). The volume over which the strain energy density is averaged is then a circular area Ω of radius R_0 centred at the notch tip, symmetric with respect to the notch bisector (Fig. 4), and the stress



distributions are those by Williams [18], written according to Lazzarin and Tovo formulation ([19]). Dealing with sharp V-notches the strain energy density averaged over the area \mathcal{Q} turns out to be:

$$\bar{W} = \frac{e_1}{E} \left[\frac{K_1}{R_0^{1-\lambda_1}} \right]^2 + \frac{e_2}{E} \left[\frac{K_2}{R_0^{1-\lambda_2}} \right]^2 \quad (1)$$

Where E is the Young's modulus of the material, λ_1 and λ_2 are Williams' eigenvalues [18], e_1 and e_2 are two parameters dependent on the notch opening angle $2a$ and on the hypothesis of plane strain or plane stress considered. Those parameters are listed in Tab. 1 as a function of the notch opening angle $2a$, for a value of the Poisson's ratio $\nu = 0.3$ and plane strain hypothesis. K_1 and K_2 are the Notch Stress Intensity Factors (NSIFs) according to Gross and Mendelson [20]:

$$\begin{aligned} K_1 &= \sqrt{2\pi} \lim_{r \rightarrow 0} r^{(1-\lambda_1)} [\sigma_{\theta\theta}(r, \theta = 0)] \\ K_2 &= \sqrt{2\pi} \lim_{r \rightarrow 0} r^{(1-\lambda_2)} [\sigma_{r\theta}(r, \theta = 0)] \end{aligned} \quad (2)$$

The SED approach was then extended to blunt U- and V-notches ([21,22]), by means of the expressions obtained by Filippi et al. [23] for the stress fields ahead of blunt notches, and to the case of multiaxial loading [24], by adding the contribution of mode III.

$2a$ [rad]	γ [rad]	λ_1	λ_2	λ_3	e_1 Plane strain	e_2 Plane strain	e_3 Axis-sym.
0	π	0.5000	0.5000	0.5000	0.13449	0.34139	0.41380
$\pi/6$	$11\pi/12$	0.5014	0.5982	0.5455	0.14485	0.27297	0.37929
$\pi/3$	$5\pi/6$	0.5122	0.7309	0.6000	0.15038	0.21530	0.34484
$\pi/2$	$3\pi/4$	0.5445	0.9085	0.6667	0.14623	0.16793	0.31034
$2\pi/3$	$2\pi/3$	0.6157	1.1489	0.7500	0.12964	0.12922	0.27587
$3\pi/4$	$5\pi/8$	0.6736	1.3021	0.8000	0.11721	0.11250	0.25863

Table 2: Values of the parameters in the SED expressions valid for a Poisson's ratio $\nu = 0.3$ (Beltrami hypothesis)

It is widely demonstrated that the SED criterion is a reliable approach for the strength determination in a wide range of materials and notch geometries [25-28], in particular it has been successfully applied to the fatigue assessment of welded joints and steel V-notched specimens. Considering a planar model for the welded joints, the toe region was modelled as a sharp V-notch. A closed form relationship for the SED approach in the control volume can be employed accordingly to Eq. (1), written in terms of range of the parameters involved. In the case of an opening angle greater than 102.6° , as in transverse non-load carrying fillet welded joints (Fig. 4), only the mode I stress distribution is singular. Then the mode II contribution can be neglected, and the expression for the SED over a control area of radius R_0 , centred at the weld toe, can be easily expressed as follows:

$$\Delta \bar{W} = \frac{e_1}{E} \left[\frac{\Delta K_1}{R_0^{1-\lambda_1}} \right]^2 \quad (3)$$

The material parameter R_0 can be estimated by equating the expression for the critical value of the mean SED range of a butt ground welded joints, $\Delta \bar{W}_C = \Delta \sigma_A / 2E$, with the one obtained for a welded joint with an opening angle $2\alpha > 102.6^\circ$. The final expression for R_0 is as follows [16]:

$$R_0 = \left(\frac{\sqrt{2e_1} \Delta K_{1,A}}{\Delta \sigma_A} \right)^{\frac{1}{1-\lambda_1}} \quad (4)$$

In Eq. (4) ΔK_{1A} is the NSIF-based fatigue strength of welded joints (211 MPa.mm^{0.326} at $N_A = 5 \times 10^6$ cycles with nominal load ratio $R = 0$) and $\Delta \sigma_A$ is the fatigue strength of the butt ground welded joint (155 MPa at $N_A = 5 \times 10^6$ cycles $R = 0$) [29]. Introducing these values into Eq. (4), $R_0 = 0.28$ mm is obtained as the radius of the control volume at the weld toe for steel welded joints. For the weld root, modelled as a crack, a value of the radius $R_0 = 0.36$ mm has been obtained by [29], re-writing the SED expression for $2a = 0$. Therefore it is possible to use a critical radius equal to 0.28 mm both for toe and root failures, as an engineering approximation [29]. It is useful to underline that R_0 depends on the failure hypothesis considered: only the total strain energy density is here presented (Beltrami hypothesis), but one could also use the deviatoric strain energy density (von Mises hypothesis) ([30]).

The SED approach was applied to a large bulk of experimental data: a final synthesis based on 900 fatigue data is shown in Fig. 5 [17], including results from structural steel welded joints of complex geometries, for which fatigue failure occurs both from the weld toe or from the weld root. Also fatigue data obtained for very thin welded joints have been successfully summarized in terms of the SED ([31]).

Recently, the SED approach has been extended to the fatigue assessment of notched specimens made of Ti-6Al-4V under multiaxial loading [32] and to high temperature fatigue data of different alloys [33]–[35]. A new method to rapidly evaluate the SED value from the singular peak stress determined by means of numerical model has been presented by Meneghetti et al. [36]. Some recent applications to creep are reported in [37].

RESULTS IN TERMS OF SED

FE analyses of the transverse non-load carrying fillet welded joint have been carried out applying as remote loads on the model the experimental values used for the fatigue tests. A control volume with a radius equal to 0.28 mm was realized in the model, in order to quantify the SED value in the control volume having the characteristic size for welded structural steel. The diagram of the SED range value $\Delta \bar{W}$ versus the number of cycles to failure N was plotted in a double logarithmic scale, summarizing the fatigue data for both bare and hot-dip galvanized specimens. With the aim to perform a direct comparison, the scatter band previously proposed for welded joints made of structural steel and based on more than 900 experimental data, Fig. 5, has been superimposed to the results of the present investigation (Fig. 6). For the detailed list of the SED values for both bare and HDG specimens corresponding to the stress ranges used in the fatigue tests, please refer to the last columns of Tab. 1.

It can be noted that hot-dip galvanized specimens have a lower fatigue strength than the bare specimens, but both bare and HDG data fall within the scatter band previously proposed in the literature for welded structural steel.

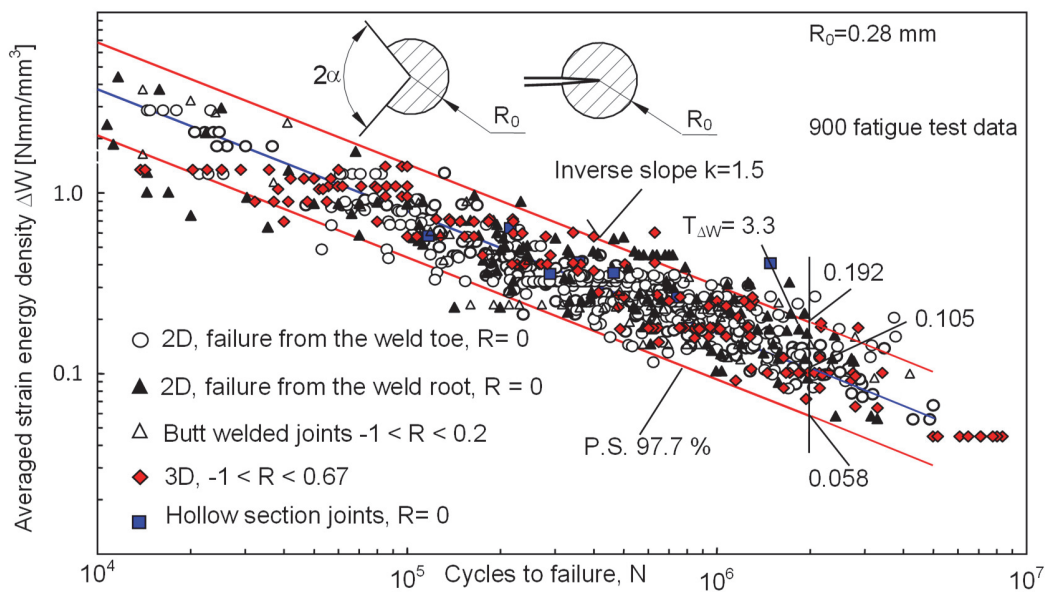


Figure 5: Fatigue strength of welded joints made of structural steel as a function of the averaged local strain energy density.

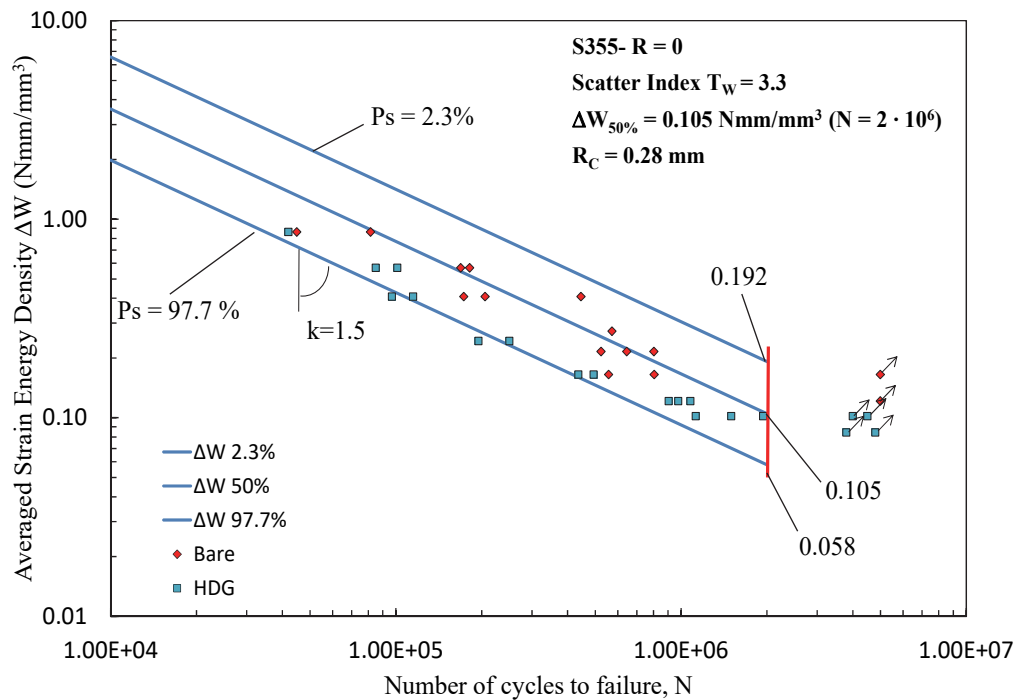


Figure 6: Fatigue behaviour of uncoated and galvanized welded steel at $R = 0$ as a function of the averaged local strain energy density. Scatter band of 900 experimental data of welded joints made of structural steel is superimposed.

ACKNOWLEDGMENTS

The authors wish to remember with great gratitude Professor Paolo Lazzarin, master of science and life, under whose leadership the research presented in this paper has been planned. Finally they want to express sincere thanks to Ing. Emiliano Guido of Zincherie Valbrenta for his active and valuable collaboration.

REFERENCES

- [1] Di Cocco, V., Sn and Ti influences on intermetallic phases damage in hot dip galvanizing, *Frattura ed Integrità Strutturale*, 22 (2012) 31-38.
- [2] Di Cocco, V., Zortea, L., Influence of dipping time on cracking during bending of hot dip galvanized coatings with Sn and Ti contents, *Frattura ed Integrità Strutturale*, 14 (2010) 52-63.
- [3] Vogt, J. B., Boussac, O., Foct, J., Prediction of fatigue resistance of a hot-dip galvanized steel, *Fatigue Fract. Eng. Mater. Struct.* 24 (2001), 33–39.
- [4] Bergengren, Y., Melander, A., An experimental and theoretical study of the fatigue properties of hot- dip-galvanized high-strength sheet steel, *Int. J. Fatigue*, 14 (1992) 154–162.
- [5] Browne, R. S., Gregory, N., Harper, S., The effects of galvanizing on the fatigue strengths of steels and welded joints, *Proceedings of a Seminar on Galvanizing of Silicon-Containing Steels*, (1975) 246 – 264.
- [6] Nilsson, T., Engberg, G., Trogen, H., Fatigue properties of hot-dip galvanized steels, *Scand. J. Metall.*, 18 (1989) 166-175.
- [7] Jiang, J. H., Ma, A. B., Weng, W. F., Fu, G. H., Zhang, Y. F., Liu, G. G., Lu, F. M., Corrosion fatigue performance of pre-split steel wires for high strength bridge cables, *Fatigue Fract Eng M*, 32 (2009) 769–779.
- [8] Yang, W. J., Yang, P., Li, X. M., Feng, W. L., Influence of tensile stress on corrosion behaviour of high-strength galvanized steel bridge wires in simulated acid rain, *Mater Corros*, 63 (2012) 401–407.
- [9] Berchem, K., Hocking, M. G., The influence of pre-straining on the high-cycle fatigue performance of two hot-dip



- galvanised car body steels, *Mater. Charact.*, 58 (2007) 593–602.
- [10] Maaß, P., Peißker, P., *Handbook of Hot-Dip Galvanization*, Wiley-VCH Verlag GmbH & Co. KGaA, Weinheim, (2011).
- [11] Valtinat, G., Huhn, H., Bolted connections with hot dip galvanized steel members with punched holes, *Proceedings of Connections in Steel Structures V*, (2004) 297–310.
- [12] Lazzarin, P., Comportamento a fatica dei giunti saldati in funzione della densità di energia di deformazione locale: influenza dei campi di tensione singolari e non singolari, *Frattura ed Integrità Strutturale*, 9 (2009) 13-26.
- [13] Maragoni, L., Carraro, P. A., Peron, M., Quaresimin, M., Fatigue behaviour of glass/epoxy laminates in the presence of voids, *Int. J. Fatigue*, 95 (2017) 18–28.
- [14] Brotzu, A., Felli, F., Pilone, D., Effects of the manufacturing process on fracture behaviour of cast TiAl intermetallic alloys, *Frattura ed Integrità Strutturale*, 27 (2013) 66-73.
- [15] Nilsson, T., Engberg, G., Trogen, H., Fatigue properties of hot-dip galvanized steels, *Scand. J. Metall.*, 18 (1989) 166–175.
- [16] Lazzarin, P., Zambardi, R., A finite-volume-energy based approach to predict the static and fatigue behavior of components with sharp V-shaped notches, *Int. J. Fract.*, 112 (2001) 275–298.
- [17] Berto, F., Lazzarin, P., Recent developments in brittle and quasi-brittle failure assessment of engineering materials by means of local approaches, *Mater. Sci. Eng. R.*, 75 (2014) 1–48.
- [18] Williams, M. L., Stress singularities resulting from various boundary conditions in angular corners on plates in extension, *J. Appl. Mech.*, 19 (1952) 526–528.
- [19] Lazzarin, P., Tovo, R., A notch intensity factor approach to the stress analysis of welds, *Fatigue Fract. Eng. Mater. Struct.*, 21 (1998) 1089–1103.
- [20] Gross, B., Mendelson, A., Plane elastostatic analysis of V-notched plates, *Int. J. Fract. Mech.* 8 (1972), 267–276.
- [21] Lazzarin, P., Berto, F., Elices, M., Gómez, J., Brittle failures from U- and V-notches in mode I and mixed, I + II, mode: A synthesis based on the strain energy density averaged on finite-size volumes, *Fatigue Fract. Eng. M.*, 32 (2009) 671–684.
- [22] Lazzarin, P., Berto, F., Some expressions for the strain energy in a finite volume surrounding the root of blunt V-notches, *Int. J. Fracture*, 135 (2005) 161–185.
- [23] Filippi, S., Lazzarin, P., Tovo, R., Developments of some explicit formulas useful to describe elastic stress fields ahead of notches in plates, *Int. J. Solids Struct.*, 39 (2002) 4543–4565.
- [24] Lazzarin, P., Livieri, P., Berto, F., Zappalorto, M., Local strain energy density and fatigue strength of welded joints under uniaxial and multiaxial loading, *Eng. Fract. Mech.*, 75 (2008) 1875–1889.
- [25] Berto, F., Lazzarin, P., Ayatollahi, M. R., Brittle fracture of sharp and blunt V-notches in isostatic graphite under torsion loading, *Carbon N. Y.*, 50 (2012) 1942–1952.
- [26] Berto, F., Ayatollahi, M. R., Fracture assessment of Brazilian disc specimens weakened by blunt V-notches under mixed mode loading by means of local energy, *Mater. Des.*, 32 (2011) 2858–2869.
- [27] Berto, F., Croccolo, D., Cuppini, R., Fatigue strength of a fork-pin equivalent coupling in terms of the local strain energy density, *Mater. Des.*, 29 (2008) 1780–1792.
- [28] Berto, F., Barati, E., Fracture assessment of U-notches under three point bending by means of local energy density, *Mater. Des.*, 32 (2011) 822–830.
- [29] Livieri, P., Lazzarin, P., Fatigue strength of steel and aluminium welded joints based on generalised stress intensity factors and local strain energy values, *Int. J. Fract.*, 133 (2005) 247–276.
- [30] Lazzarin, P., Lassen, T., Livieri, P., A notch stress intensity approach applied to fatigue life predictions of welded joints with different local toe geometry, *Fatigue Fract. Eng. M.*, 26 (2003) 49–58.
- [31] Lazzarin, P., Berto, F., Atzori, B., A synthesis of data from steel spot welded joints of reduced thickness by means of local SED, *Theor. Appl. Fract. Mec.*, 63-64 (2013) 32–39.
- [32] Berto, F., Campagnolo, A., Lazzarin, P., Fatigue strength of severely notched specimens made of Ti-6Al-4V under multiaxial loading, *Fatigue Fract. Eng. Mater. Struct.*, 38 (2015) 503–517.
- [33] Gallo, P., Berto, F., Lazzarin, P., High temperature fatigue tests of notched specimens made of titanium Grade 2, *Theor. Appl. Fract. Mech.*, 76 (2015) 27–34.
- [34] Berto, F., Gallo, P., Lazzarin, P., High temperature fatigue tests of a Cu-Be alloy and synthesis in terms of linear elastic strain energy density, *Key Eng. Mater.*, 627 (2015) 77–80.
- [35] Gallo, P., Berto, F., Influence of surface roughness on high temperature fatigue strength and cracks initiation in 40CrMoV13.9 notched components, *Theor. Appl. Fract. Mech.*, 80 (2015) 226–234.



- [36] Meneghetti, G., Campagnolo, A., Berto, F., Atzori, B., Averaged strain energy density evaluated rapidly from the singular peak stresses by FEM: cracked components under mixed-mode (I+II) loading, *Theor. Appl. Fract. Mech.*, 79 (2015) 113–124.
- [37] Gallo, P., Berto, F., Glinka, G Generalized approach to estimation of strains and stresses at blunt V-notches under non-localized creep, *Fatigue Fract. Eng. Mater. Struct.*, 39 (2016) 292-306.

NOMENCLATURE

$2a$	notch opening angle
γ	supplementary angle of α : $\gamma = \pi - \alpha$
ν	Poisson's ratio
$\Delta\sigma$	stress range
$\Delta\sigma_A$	fatigue strength in terms of stress range at N_A cycles
$\Delta K_{1,2,3}$	mode 1, 2 and 3 notch stress intensity factor range
$\Delta K_{1,A}$	fatigue strength in terms of notch stress intensity factor range at N_A cycles
$\Delta\bar{W}$	averaged strain energy density (SED)
$\Delta\bar{W}_C$	critical value of the SED range
$\lambda_{1,2,3}$	mode 1, 2 and 3 Williams' eigenvalues
E	Young's modulus
$e_{1,2,3}$	mode 1, 2 and 3 functions in the SED expression
f	frequency
$K_{1,2,3}$	mode 1, 2 and 3 notch stress intensity factor (NSIF)
k	inverse slope of the Wöhler curve
N	number of cycles
P_s	survival probability
R	load cycle ratio
R_0	radius of the control volume for the calculation of the averaged SED value
T_σ	scatter index referred to the stress range
T_W	scatter index referred to the SED range